

AD-A113 852

VIRGINIA POLYTECHNIC INST AND STATE UNIV BLACKSBURG --ETC F/8 11/7
GEOMETRICALLY NONLINEAR TRANSIENT ANALYSIS OF LAMINATED COMPOSI--ETC(U)
MAR 82 J N REDDY AFOSR-81-0142

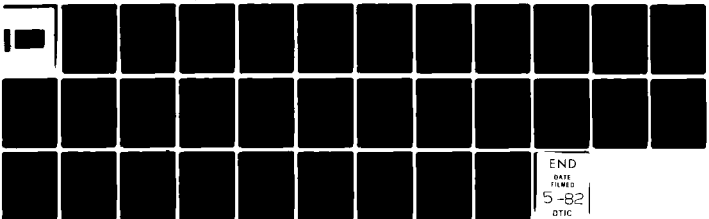
UNCLASSIFIED

VPI-E-82.8

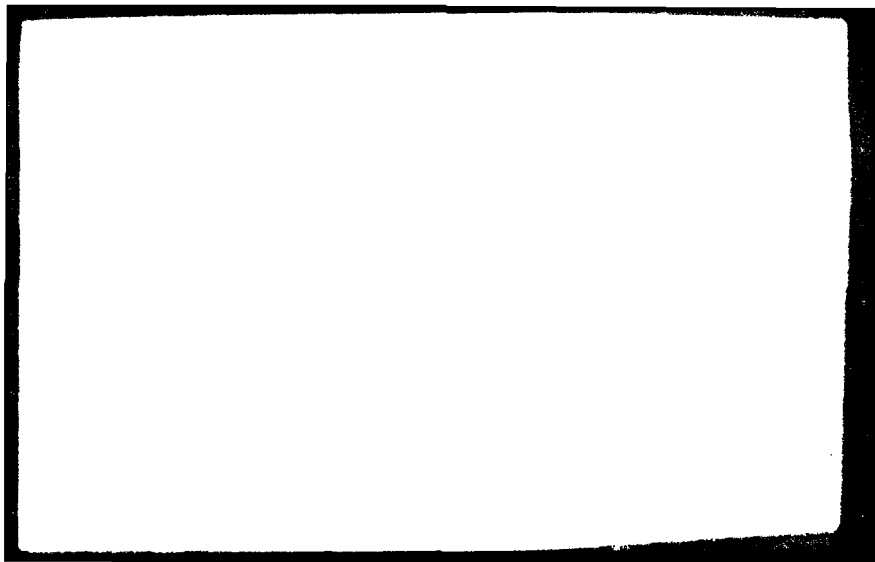
AFOSR-TR-81-3

NL

Fig 1
0.6
0.3sec



END
DATE
FILMED
5-82
DTIC



12

The United States Air Force
AIR FORCE OFFICE OF SCIENTIFIC RESEARCH
Structural Mechanics Program
Bolling AFB, D. C. 20332

Grant No. AFOSR-81-0142
Technical Report No. AFOSR-81-3

VPI-E-82.8

GEOMETRICALLY NONLINEAR TRANSIENT ANALYSIS OF
LAMINATED COMPOSITE PLATES

J. N. Reddy

Department of Engineering Science and Mechanics
Virginia Polytechnic Institute and State University
Blacksburg, Virginia 24061

March 1982

DTIC
ELECTE
S APR 27 1982 D
E

Approved for public release; distribution unlimited

GEOMETRICALLY NONLINEAR TRANSIENT ANALYSIS OF
LAMINATED COMPOSITE PLATES

J. N. Reddy†
Virginia Polytechnic Institute and State University
Blacksburg, Virginia 24061

Abstract

Forced motions of laminated composite plates are investigated using a finite element that accounts for the transverse shear strains, rotary inertia, and large rotations (in the von Karman sense). The present results when specialized for isotropic plates are found to be in good agreement with those available in the literature. Numerical results of the nonlinear analysis of composite plates are presented showing the effects of plate thickness, lamination scheme, boundary conditions, and loading on the deflections and stresses. The new results for composite plates should serve as bench marks for future investigations.

Nomenclature

A_{ij}, B_{ij}, D_{ij} extensional, flexural-extensional and flexural stiffnesses ($i, j = 1, 2, 6$).

a, b plate planform dimensions of x, y directions,

$a_0, a_1, \text{ etc.}$ parameters in the time approximation (see eqn.(15))

E_1, E_2 layer elastic moduli in directions along fibers and normal to them, respectively

G_{12}, G_{13}, G_{23} layer inplane and thickness shear moduli

h total thickness of the plate

By _____	
Distribution/	
Availability Codes	
Dist	Avail and/or Special
A	

†Professor, Department of Engineering Science and Mechanics.



I	rotatory inertia coefficient per unit midplane area of layer
k_i	shear correction coefficients associated with the yz and xz planes, respectively ($i = 4,5$)
M_i, N_i	stress couple and stress resultant, respectively ($i=1,2,6$)
P	laminate normal inertia coefficient per unit midplane area
Q_i	shear stress resultant ($i = 1,2$)
Q_{ij}	plane-stress reduced stiffness coefficients ($i,j = 1,2,6$)
R	laminate rotatory-normal coupling inertia coefficient per unit midplane area
u, v, w	displacement components in x, y, z directions, respectively
U_i, V_i, W_i	nodal values of displacements u, v, w ($i = 1, 2, \dots, n$)
x, y, z	position coordinates in cartesian system
$\{\Delta\}$	column vector of generalized nodal displacements
α, β	parameters in the Newmark integration scheme
ϵ_i	strain components ($i = 1, 2, \dots, 6$)
θ_m	orientation of m -th layer ($m = 1, 2, \dots, L$)
$\rho^{(m)}$	density of m -th layer ($m = 1, 2, \dots, L$)
σ_i	stress components ($i = 1, 2, \dots, 6$)
ϕ_i	finite-element interpolation functions ($i = 1, 2, \dots, n$)
ϕ_x, ϕ_y	bending slope (rotation) functions

Introduction

The transient behavior of isotropic and homogeneous plates has long been a subject of interest (see Lamb¹ for thin plates and David and Lawhead² for thick plates). For many years, the classical (Poisson-Kirchoff) plate theory (CPT), in which normals to the midsurface before deformation are assumed to remain straight and normal to the midsurface after deformation (i.e., transverse shear strains are zero), has been used to calculate frequencies, static response, and dynamic response under applied loads. Recent studies in the analysis of plates have shown that the effect of the transverse shear strains on the static and dynamic response of plates is significant. For example, the natural frequencies of vibration predicted by the classical plate theory are 25% higher, for plate side-to-thickness ratio of 10, than those predicted by a shear deformation theory (SDT). In transient analysis of plates the classical plate theory predicts unrealistically large phase velocities in the plate for shorter wave lengths. The Timoshenko beam theory³, which includes transverse shear and rotary inertia effects, has been extended to isotropic plates by Reissner^{4,5} and Mindlin⁶, and to laminated anisotropic plates by Yang, Norris, and Stavsky⁷. A generalization of the von Karman nonlinear plate theory for isotropic plates to include the effects of transverse shear and rotary inertia in the theory of orthotropic plates is due to Medwadowski⁸, and that for anisotropic plates is due to Ebcioğlu⁹.

With the increased application of advanced fiber composite materials to jet engine fan or compressor blades, and in high performance aircraft, studies involving transient response of plates made of such materials are needed to assess the ability of these

materials to withstand the forces of impact due to foreign objects (e.g., the ingestion of stones, nuts, and bolts, hailstones, or birds in jet engines). Previous investigations into the linear transient analysis of composite plates include Moon's^{10,11} investigation of the response of infinite laminated plates subjected to transverse impact loads at the center of the plate; Chow's¹² study of laminated plates (with transverse shear and rotary inertia) using the Laplace transform technique; Wang, Chou, and Rose's¹³ investigation, by the method of characteristics, of unsymmetrical orthotropic laminated plates; and Sun and Whitney's^{14,15} study of plates under cylindrical bending. More recently, the present author^{16,17} investigated the linear transient response of layered anisotropic composite rectangular plates and presented extensive numerical results for center deflection and stresses.

Geometrically nonlinear transient analysis of isotropic plates was considered by Hinton, et al.¹⁸⁻²⁰ and Akay²¹. Hinton, et al. used the Mindlin element while Akay used a mixed finite element in their works. As far as the nonlinear (geometric) analysis of layered anisotropic composite plates is concerned, there exist no previously reported results in the open literature. The present investigation is concerned with the geometrically nonlinear transient analysis of layered composite plates under applied transverse loads. The shear deformable element developed by the author¹⁷ for the transient analysis of layered composite plates is modified to include the nonlinear strain-displacement relations of the von Karman plate theory. Numerical results are presented to show the effect of lamination scheme, plate thickness, nonlinearity, boundary conditions, and loading on the

transient response of plates. The numerical results included here for layered composite plates are not available in the literature, and therefore should be of interest to designers of composite-plate structures and numerical analysts and experimentalists in evaluating their techniques.

Review of the Equations of Motion of Anisotropic Plates

The nonlinear theory of laminated anisotropic plates to be reviewed is based on the combination of the Timoshenko-type theory and the von Karman plate theory. The theory is known to be able to predict accurately the global behavior. However, it is not accurate enough to predict edge stresses and hence delamination. The theory assumes that the stresses normal to the midplane of the plate are negligible when compared to the inplane stresses, and normals to the plate midsurface before deformation remain straight but not necessarily normal to the midsurface after deformation.

Equations of motion

The plate under consideration is composed of a finite number of orthotropic layers of uniform thickness, with principal axes of elasticity oriented arbitrarily with respect to the plate axes. The x and y -coordinates of the plate are taken in the midplane (Ω) of the plate. As in all Timoshenko-type theories, the displacement field is assumed to be of the form

$$u_1(x,y,z,t) = u(x,y,t) + z\phi_x(x,y,t),$$

$$u_2(x,y,z,t) = v(x,y,t) + z\phi_y(x,y,t), \quad (1)$$

$$u_3(x,y,z,t) = w(x,y,t).$$

Here t is the time; u_1, u_2, u_3 are the displacements in the x, y, z directions, respectively; u, v, w are the associated midplane displacements; and ϕ_x and ϕ_y are the slopes in the xz and yz planes due to bending only. The strains in the von Karman plate theory (which accounts for moderately large deflections and small strains) can be expressed in the form

$$\begin{aligned}\epsilon_1 &= \frac{\partial u}{\partial x} + \frac{1}{2} \left(\frac{\partial w}{\partial x}\right)^2 + z \frac{\partial \phi_x}{\partial x} \equiv \epsilon_1^0 + z\kappa_1 \\ \epsilon_2 &= \frac{\partial v}{\partial y} + \frac{1}{2} \left(\frac{\partial w}{\partial y}\right)^2 + z \frac{\partial \phi_y}{\partial y} \equiv \epsilon_2^0 + z\kappa_2 \\ \epsilon_6 &= \frac{\partial u}{\partial y} + \frac{\partial v}{\partial x} + \frac{\partial w}{\partial x} \frac{\partial w}{\partial y} + z \left(\frac{\partial \phi_x}{\partial y} + \frac{\partial \phi_y}{\partial x}\right) \equiv \epsilon_6^0 + z\kappa_6 \\ \epsilon_5 &= \phi_x + \frac{\partial w}{\partial x}, \quad \epsilon_4 = \phi_y + \frac{\partial w}{\partial y}\end{aligned}\tag{2}$$

wherein the squares of the first spatial derivatives of u, v, ϕ_x and ϕ_y are neglected. The strain ϵ_3 does not enter the equations because the constitutive relations, to be given shortly, are based on the plane-stress assumption. Note that the transverse shear strains, ϵ_4 and ϵ_5 , are constant through the thickness. If a linear distribution of the transverse shear strains through the thickness is desired, one must add higher order terms in z to the displacements u_1 and u_2 , and/or u_3 ; with each additional term, an additional dependent variable is introduced into the problem.

Neglecting the body moments and surface shearing forces, we write the equations of motion in the presence of applied transverse forces, q , as

$$\begin{aligned}
N_{1,x} + N_{6,y} &= Pu_{,tt} + R\phi_{x,tt} \\
N_{6,x} + N_{2,y} &= Pv_{,tt} + R\phi_{y,tt} \\
Q_{1,x} + Q_{2,y} &= Pw_{,tt} + q(x,y,t) + N(w,N_i)
\end{aligned} \tag{3}$$

$$M_{1,x} + M_{6,y} - Q_1 = I\phi_{x,tt} + Ru_{,tt}$$

$$M_{6,x} + M_{2,y} - Q_2 = I\phi_{y,tt} + Rv_{,tt}$$

where P , R and I are the normal, coupled normal-rotary, and rotary inertia coefficients,

$$(P,R,I) = \int_{-h/2}^{h/2} (1,z,z^2)\rho dz = \sum_m \int_{z_m}^{z_{m+1}} (1,z,z^2)\rho^{(m)} dz \tag{4}$$

$\rho^{(m)}$ being the material density of the m -th layer, N_i , Q_i , and M_i are the stress and moment resultants defined by

$$(N_i, M_i) = \int_{-h/2}^{h/2} (1,z)\sigma_i dz, \quad (Q_1, Q_2) = \int_{-h/2}^{h/2} (\sigma_5, \sigma_4) dz, \tag{5}$$

and $N(w, N_i)$ is the contribution due to the nonlinear terms,

$$N(w, N_i) = \frac{\partial w}{\partial x} \left(\frac{\partial N_1}{\partial x} + \frac{\partial N_6}{\partial y} \right) + \frac{\partial w}{\partial y} \left(\frac{\partial N_6}{\partial x} + \frac{\partial N_2}{\partial y} \right) \tag{6}$$

Here σ_i ($i = 1, 2, \dots, 6$) denote the in-plane stress components

($\sigma_1 = \sigma_x$, $\sigma_2 = \sigma_y$, $\sigma_4 = \sigma_{zy}$, $\sigma_5 = \sigma_{xz}$ and $\sigma_6 = \sigma_{xy}$).

If one plane of elastic symmetry parallel to the plane of each layer exists, the constitutive equations for the plate can be written in the form (see Jones²²),

$$\begin{Bmatrix} N_i \\ M_i \end{Bmatrix} = \begin{bmatrix} A_{ij} & B_{ij} \\ B_{ji} & D_{ij} \end{bmatrix} \begin{Bmatrix} \epsilon_j^0 \\ \kappa_j \end{Bmatrix}, \quad \begin{Bmatrix} Q_2 \\ Q_1 \end{Bmatrix} = \begin{bmatrix} \bar{A}_{44} & \bar{A}_{45} \\ \bar{A}_{45} & \bar{A}_{55} \end{bmatrix} \begin{Bmatrix} \epsilon_4 \\ \epsilon_5 \end{Bmatrix} \tag{7}$$

The A_{ij} , B_{ij} , D_{ij} ($i, j = 1, 2, 6$), and \bar{A}_{ij} ($i, j = 4, 5$) are the inplane, bending-inplane coupling, bending or twisting, and thickness-shear stiffnesses, respectively:

$$(A_{ij}, B_{ij}, D_{ij}) = \sum_m \int_{z_m}^{z_{m+1}} Q_{ij}^{(m)} (1, z, z^2) dz, \quad \bar{A}_{ij} = \sum_m \int_{z_m}^{z_{m+1}} k_i k_j Q_{ij}^{(m)} dz \quad (8)$$

Here z_m denotes the distance from the mid-plane to the lower surface of the m -th layer, and k_i are the shear correction coefficients.

Variational Formulation

The variational form of Eqs. (3) and (7) is given by

$$\begin{aligned} 0 = & \int_{\Omega} \{ \delta u (P u_{,tt} + R \phi_{x,tt}) + \delta u_{,x} N_1 + \delta u_{,y} N_6 + \delta v (P v_{,tt} + R \phi_{y,tt}) \\ & + \delta v_{,x} N_6 + \delta v_{,y} N_2 + \delta w (P w_{,tt}) + \delta w_{,x} Q_1 + \delta w_{,y} Q_2 \\ & + \frac{\partial \delta w}{\partial x} \left(\frac{\partial w}{\partial x} N_1 + \frac{\partial w}{\partial y} N_6 \right) + \frac{\partial \delta w}{\partial y} \left(\frac{\partial w}{\partial x} N_6 + \frac{\partial w}{\partial y} N_2 \right) \\ & + \delta \phi_x (I \phi_{x,tt} + R u_{,tt}) + \delta \phi_{x,x} M_1 + \delta \phi_{x,y} M_6 + \delta \phi_x Q_1 \\ & + \delta \phi_y (I \phi_{y,tt} + R v_{,tt}) + \delta \phi_{y,x} M_6 + \delta \phi_{y,y} M_2 + \delta \phi_y Q_2 + \delta w q \} dx dy \\ & + \int_{\Gamma} (\delta u_n N_n + \delta u_s N_{ns}) ds + \int_{\Gamma} \delta w V ds + \int_{\Gamma} (\delta \phi_n M_n + \delta \phi_s M_{ns}) ds, \end{aligned} \quad (9)$$

wherein N_i , M_i and Q_i are given in terms of the generalized displacements by Eq. (7), and V , N_n and N_{ns} , and M_n and M_{ns} are the shear force, normal and tangential in-plane forces, and normal and twisting bending moments defined on the boundary Γ , respectively:

$$V = Q_1 n_x + Q_2 n_y + \left(\frac{\partial w}{\partial x} N_1 + \frac{\partial w}{\partial y} N_6 \right) n_x + \left(\frac{\partial w}{\partial x} N_6 + \frac{\partial w}{\partial y} N_2 \right) n_y$$

$$\begin{aligned}
N_n &= n_x n_x N_1 + 2n_x n_y N_6 + n_y n_y N_2 \\
N_{ns} &= n_x n_y (N_2 - N_1) + (n_x n_x - n_y n_y) N_6 \\
M_n &= n_x n_x M_1 + 2n_x n_y M_6 + n_y n_y M_2 \\
M_{ns} &= n_x n_y (M_2 - M_1) + (n_x n_x - n_y n_y) M_6,
\end{aligned} \tag{10}$$

where $\hat{n} = (n_x, n_y)$ is the unit vector normal to the boundary Γ . The variational formulation indicates that the essential (i.e., geometric) and natural boundary conditions of the problem are given by:

$$\begin{aligned}
\text{essential} & \text{ specify: } u_n, u_s, w, \phi_n, \phi_s \\
\text{natural} & \text{ specify: } N_n, N_{ns}, V, M_n, M_{ns}.
\end{aligned} \tag{11}$$

wherein u_n and u_s , for example, denote the normal and tangential components of the inplane displacement vector, $\underline{u} = (u, v)$.

A Shear-Deformable Finite-Element for Laminated Plates

Here we present a finite-element model associated with the nonlinear equations governing the motion of layered composite plates. The element is an extension of the penalty plate-bending element developed for the linear static and dynamic analysis of layered composite plates by the present author^{17,23}.

Consider a finite-element analog, Ω_h , of the midplane of the plate, Ω . Over a typical element, Ω_e of the mesh Ω_h , each generalized displacement U is interpolated spatially by an expression of the form,

$$U = \sum_i^r U_i(t) \phi_i(x, y) \tag{12}$$

where U_i is the value of U at node i at time t , ϕ_i is the finite-element interpolation function at node i and r is the number of nodes in the element. For the sake of simplicity, we use the same interpolation function for each of the generalized displacements, $(u, v, w, \phi_x, \phi_y)$. Specifically, the nine-node isoparametric rectangular element with five degrees of freedom is used in the present study.

Substituting Eqs. (7) and (12) into Eq. (9), we obtain the following equation:

$$[K]\{\Delta\} + [M]\{\ddot{\Delta}\} = \{F\} \quad (13)$$

Here $\{\Delta\}$ is the column vector of the nodal values of the generalized displacements, $[K]$ is the matrix of stiffness coefficients, $[M]$ is the matrix of mass coefficients, and $\{F\}$ is the column vector containing the boundary and transverse force contributions. The elements of $[K]$ and $[M]$ are given in Appendix A.

It should be pointed out that the element stiffness matrix $[K]$ is nonlinear and unsymmetric in the present formulation (see Appendix A), the nonlinearity being due to the nonlinear terms appearing in the variational formulation. The nonsymmetric nature of the stiffness matrix needs some explanation. To this end consider the following terms from the variational formulation,

$$\dots + A_{11} \frac{\partial \delta u}{\partial x} \left[\frac{\partial u}{\partial x} + \frac{1}{2} \left(\frac{\partial w}{\partial x} \right)^2 \right] + A_{11} \frac{\partial \delta w}{\partial x} \frac{\partial w}{\partial x} \left[\frac{\partial u}{\partial x} + \frac{1}{2} \left(\frac{\partial w}{\partial x} \right)^2 \right] + \dots$$

The first term contributes to the stiffness coefficients K_{ij}^{11} and K_{ij}^{13} (see Appendix A), whereas the second term contributes to the stiffness coefficients K_{ij}^{31} and K_{ij}^{33} . Note that

$$K_{ij}^{13} = \int_{\Omega^e} A_{11} \left(\frac{1}{2} \frac{\partial w}{\partial x} \right) \frac{\partial \phi_i}{\partial x} \frac{\partial \phi_j}{\partial x} dx dy + \dots$$

$$K_{ij}^{31} = \int_{\Omega^e} A_{11} \left(\frac{\partial w}{\partial x} \right) \frac{\partial \phi_i}{\partial x} \frac{\partial \phi_j}{\partial x} dx dy + \dots$$

are not the same.

To complete the discretization, we must now approximate the time derivatives appearing in Eq. (13). Here we use the Newmark direct integration method²⁴, with $\alpha = 0.5$ and $\beta = 0.25$ (corresponding to the constant-average-acceleration method). The scheme, although unconditionally stable for linear problems, is not proved to be stable for nonlinear problems.

Equation (13) can be expressed, after the application of Newmark's integration scheme, in the form

$$[\hat{K}]\{\Delta\}_{n+1} = \{\hat{F}\}_{n,n+1} \quad (14)$$

where

$$\begin{aligned} [\hat{K}] &= [K] + a_0[M], \quad \{\hat{F}\} = \{F\}_{n+1} + [M](a_0\{\Delta\}_n + a_1\{\dot{\Delta}\}_n + a_2\{\ddot{\Delta}\}_n), \\ a_0 &= 1/(\beta\Delta t^2), \quad a_1 = a_0\Delta t, \quad a_2 = \frac{1}{2\beta} - 1. \end{aligned} \quad (15)$$

Once the solution $\{\Delta\}$ is known at $t_{n+1} = (n+1)\Delta t$, the first and second derivatives (velocity and accelerations) of $\{\Delta\}$ at t_{n+1} can be computed from

$$\begin{aligned} \{\ddot{\Delta}\}_{n+1} &= a_0(\{\Delta\}_{n+1} - \{\Delta\}_n) - a_1\{\dot{\Delta}\}_n - a_2\{\ddot{\Delta}\}_n \\ \{\dot{\Delta}\}_{n+1} &= \{\dot{\Delta}\}_n + a_3\{\ddot{\Delta}\}_n + a_4\{\ddot{\Delta}\}_{n+1} \end{aligned} \quad (16)$$

where $a_3 = (1 - \alpha)\Delta t$, and $a_4 = \alpha\Delta t$.

All of the operations indicated above (except for eqn. (16)) can be performed at the element level, and the assembled form of eqn. (14) can be obtained for the whole problem:

$$[K] = [K^L + K^N(\{\Delta\}_{n+1})] \quad (17)$$

where $[K^L]$ denotes the linear stiffness matrix and $[K^N]$ denotes the nonlinear (geometric) stiffness matrix. Because $[K^N]$ depends on the unknown solution $\{\Delta\}_{n+1}$, the assembled equation must be solved iteratively until a convergence criterion is satisfied at time, $t = t_{n+1}$. In the present study the Picard type successive iteration scheme is employed. In this scheme, the nonlinear equations (14) are approximated by the following equation

$$[\hat{K}(\{\Delta^r\}_{n+1})][\Delta^{r+1}]_{n+1} = \{\hat{F}\}_{n,n+1} \quad (18)$$

where r is the iteration number. In other words, the nonlinear stiffness matrix for the $(r + 1)$ -th iteration is computed using the solution vector from the r -th iteration. Such successive iterations are continued until the error

$$E \equiv \left[\sum_{i=1}^N |\Delta_i^r - \Delta_i^{r+1}|^2 \quad \sum_{i=1}^N |\Delta_i^r|^2 \right] \quad (19)$$

for any fixed time $t = t_{n+1}$, is less than or equal to some preassigned value (say, one percent or less). The iteration at time $t = t_{n+1}$ is started by using the converged solution at $t = t_n$ (at $t = t_0 \equiv 0$, the initial conditions are assumed to be known).

Numerical Results and Discussion

In the present study the nine-node rectangular isoparametric element was employed. The element has either three (w, ψ_x, ψ_y) or five (u, v, w, ψ_x, ψ_y) degrees of freedom (DOF) per node. Because the element accounts for the transverse shear strains, reduced integration was employed to evaluate the shear terms numerically. In other words, the 2x2 Gauss rule was used to integrate the shear energy terms and the 3x3 Gauss rule was used to integrate the bending and inertia terms. All computations were done in double precision on an IBM 3032. Due to the biaxial symmetry of the problems discussed, only one quadrant of the plate was analyzed. In all of the numerical examples considered here, zero initial conditions are assumed and damping is neglected.

Because no estimate on the time step for the nonlinear analysis is available in the literature, the critical time step of a conditionally stable finite difference scheme was used as a starting time step, and a convergence study was conducted to select a time step that yielded a stable and accurate solution while keeping the computational time to a minimum. The following two estimates were used in the present study:

$$\Delta t_1 < 0.25 (\rho h D)^{1/2} (\Delta x)^2 \quad (20)$$

$$\Delta t_2 < [\rho(1 - \nu^2)E / \{2 + 11 - \nu\} \frac{\pi^2}{12} [1 + 1.5 (\frac{\Delta x}{h})^2]]^{1/2} \Delta x \quad (21)$$

Here $D = Eh^3/[12(1 - \nu^2)]$, and Δx is the minimum distance between the element node points. Estimate (20), due to Leech²⁵, was derived for thin plates, and estimate (21), due to Tsui and Pin Tong²⁶, was derived for thick plates.

First, in order to prove the validity of the present formulation, the results obtained in the present study for isotropic plates are

compared with those available in the literature:

1. Simply supported rectangular plate under suddenly applied patch loading (see Fig. 1 and Ref. [27])

$$a = \sqrt{2}, b = 1, h = 0.1 \text{ and } 0.2, \Delta t = 0.1, q = q_0 H(t)$$

$$q_0 = \begin{cases} 10^{-2}, & 0 < x, y < 0.2 \\ 0 & , x, y > 0.2 \end{cases} \quad (22)$$

$$E_1 = E_2 = 1.0, \nu_{12} = 0.3, \rho = 1.0.$$

2. Simply supported square plates under suddenly applied uniformly distributed loading (see Fig. 2 and Ref. [21])

$$a=b = 243.8 \text{ cm}, h = 0.635 \text{ cm}, \Delta t = 0.005 \text{ sec.}, q_0 = 4.882 \times 10^{-4} \text{ N/cm}^2,$$

$$E_1 = E_2 = 7.031 \times 10^5 \text{ N/cm}^2, \nu_{12} = 0.25, \rho = 2.547 \times 10^{-6} \text{ N sec}^2/\text{cm}^4.$$

(23)

3. Clamped circular plate under suddenly applied uniformly distributed loading (see Fig. 3 and Ref. [19])

$$R(\text{radius}) = 100 \text{ in.}, h = 10 \text{ and } 20 \text{ in.}, \Delta t = 2.5 \text{ sec.}, q_0 = 1.0 \text{ psi},$$

$$E_1 = E_2 = 100 \text{ psi}, \nu_{12} = 0.3, \rho = 10 \text{ lb sec}^2/\text{inch}^4. \quad (24)$$

1. Simply supported, rectangular, isotropic and orthotropic plates. A 4x4 (nonuniform) mesh is used in the quarter plate with 3 DOF per node. The center deflection and bending moments of the present linear analysis are compared with the analytical thick-plate and thin-plate solutions of Reismann and Lee²⁷ in Fig. 4. We note pronounced difference between the solutions of the two theories. The deviation between the solutions of the shear deformation theory and the classical theory increases with plate thickness. The present finite element solutions for the center deflection and bending moment are in excellent agreement with those of Reismann and Lee²⁷.

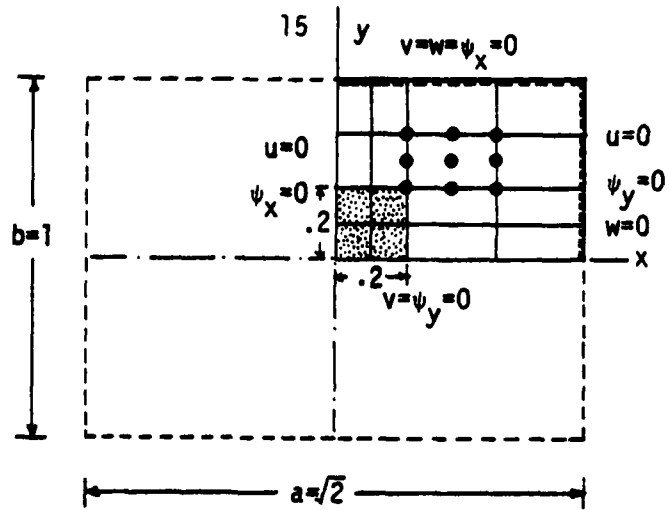
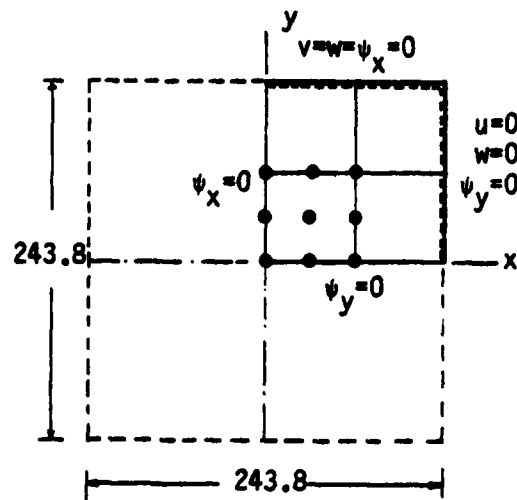


Figure 1. Finite-element mesh and boundary conditions for isotropic rectangular plates under suddenly applied pressure loading at the center.



$$\text{BC1: } u(0,y)=v(x,0)=0$$

$$\text{BC2: } u(y,0)=v(0,y)=0$$

Figure 2. Finite-element mesh and boundary conditions for isotropic square plates under suddenly applied pressure loading.

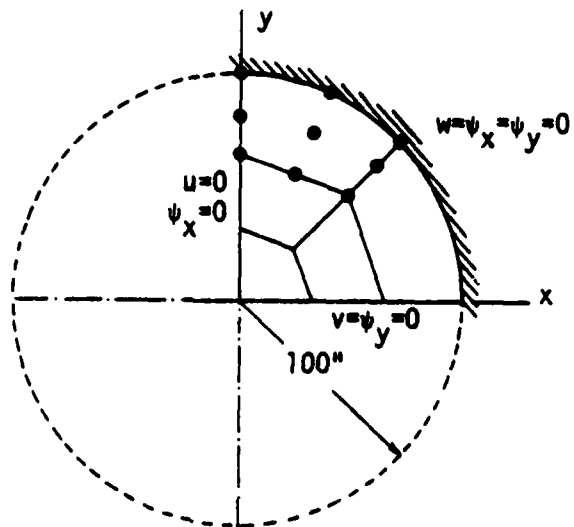


Figure 3. Finite-element mesh and boundary conditions for an isotropic clamped square plate under suddenly applied pressure loading.

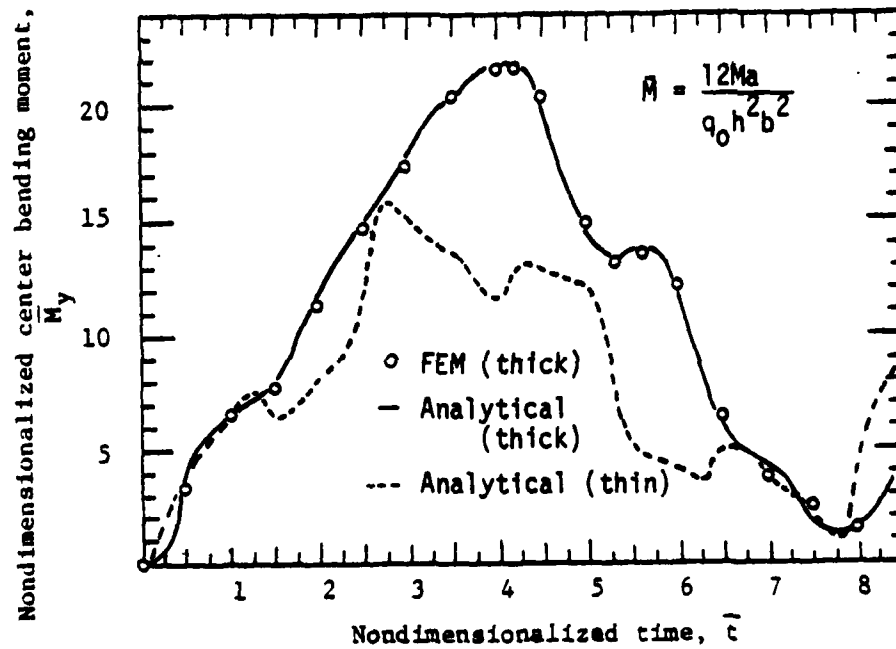
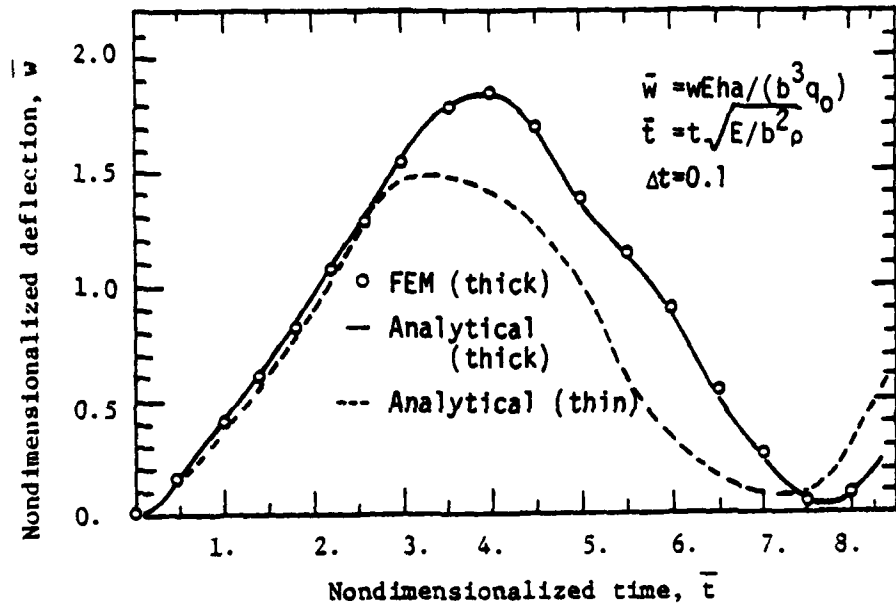


Figure 4. Nondimensionalized center deflection and bending moment versus nondimensionalized time for simply supported rectangular plates ($\nu = 0.3$) under suddenly applied pressure loading at the center square area (4x4 mesh).

The center deflections obtained in the present linear and nonlinear analysis are presented in Fig. 5. To show the effect of material orthotropy on the center deflection, results of the linear analysis of an orthotropic plate ($E_1/E_2 = 25$, $\nu_{12} = 0.25$) are also included in Fig. 5. The effect of orthotropy and geometric nonlinearity on the amplitude and period of nondimensionalized center deflection of orthotropic plates ($E_1/E_2 = 25$, $\nu_{12} = 0.25$) is apparent from the plots presented in Fig. 5; the effect of orthotropy is to decrease both amplitude and period of the center deflection, and effect of the nonlinearity is to decrease the amplitude, and smoothen the solution somewhat. The effect of the plate thickness on the amplitude and period of the nondimensionalized center deflection (linear) $\bar{w} = 10wE_2h^3/q_0h^4$, can be seen from the plots in Fig. 6. The amplitude decreased about 30% for a decrease in thickness from $\frac{b}{h} = 0.2$ to $\frac{b}{h} = 0.1$.

2. Simply-supported square plates (BC1). A 2x2 (uniform) mesh is used in the quarter plate with 5 DOF per node. Results of the present nonlinear analysis (see Fig. 7) agree closely with the mixed finite element results of Akay²¹. The plots of center deflection versus time for various loads are shown in Fig. 7 along with the load-deflection curve. Note that amplitude and period of the center deflection decrease with increasing values of the load. Further note that the negative peak also increases with decreasing load.

3. Clamped circular plates. Results of the linear transient analysis of the clamped square plate, for two different thicknesses, are presented in Figs. 8a and b. The present results agree with those reported by Hinton¹⁹. The effect of the decrease in thickness is to increase the amplitude and period of the center deflection and stress.

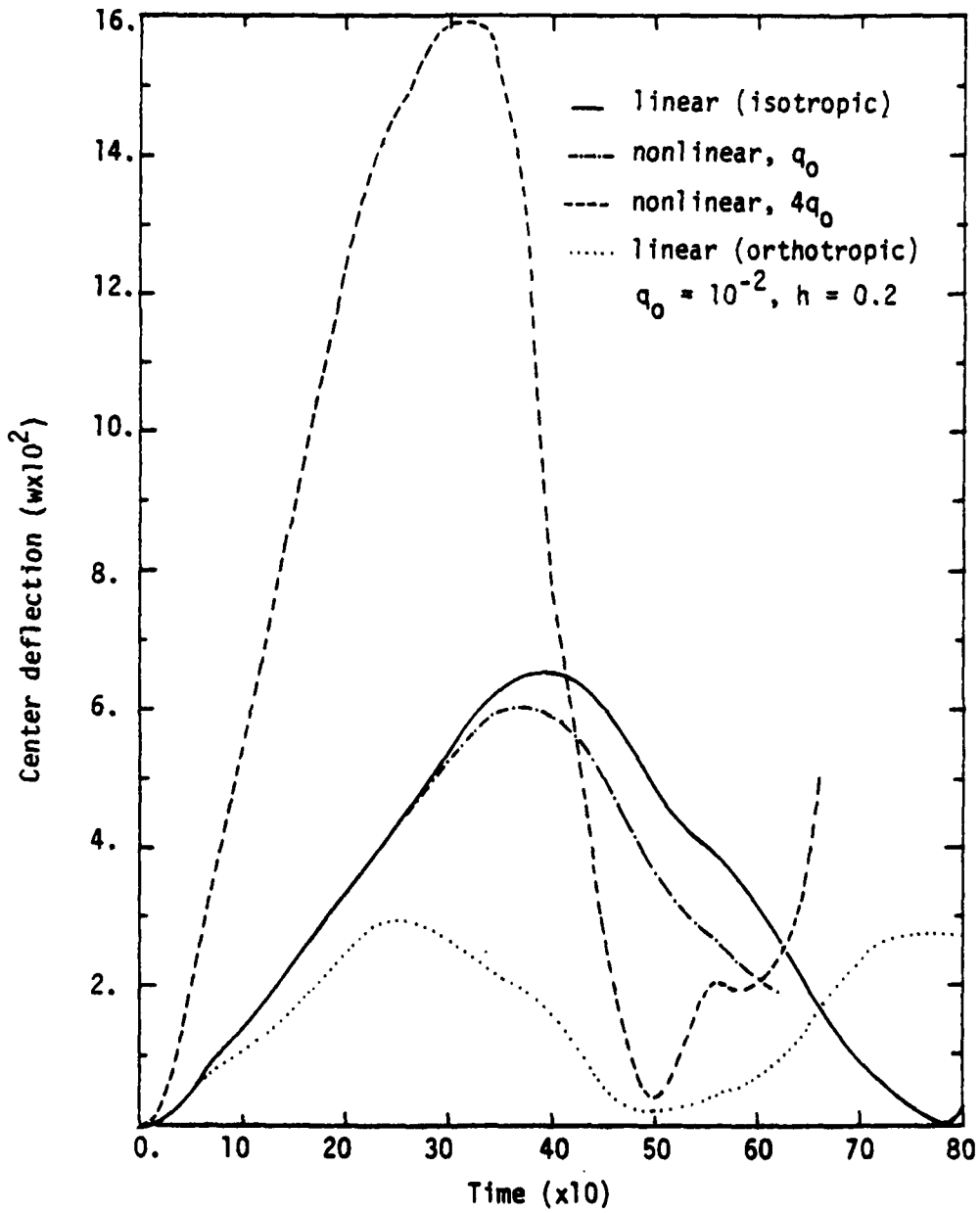


Figure 5. Center deflection versus time for isotropic (see eqn. (22)) and orthotropic ($E_1=25$, $E_2=1$, $\nu_{12}=0.25$, $G_{12}=G_{13}=G_{23}=0.5E_2$) rectangular plates under suddenly applied loading at the center square area (see Figure 1).

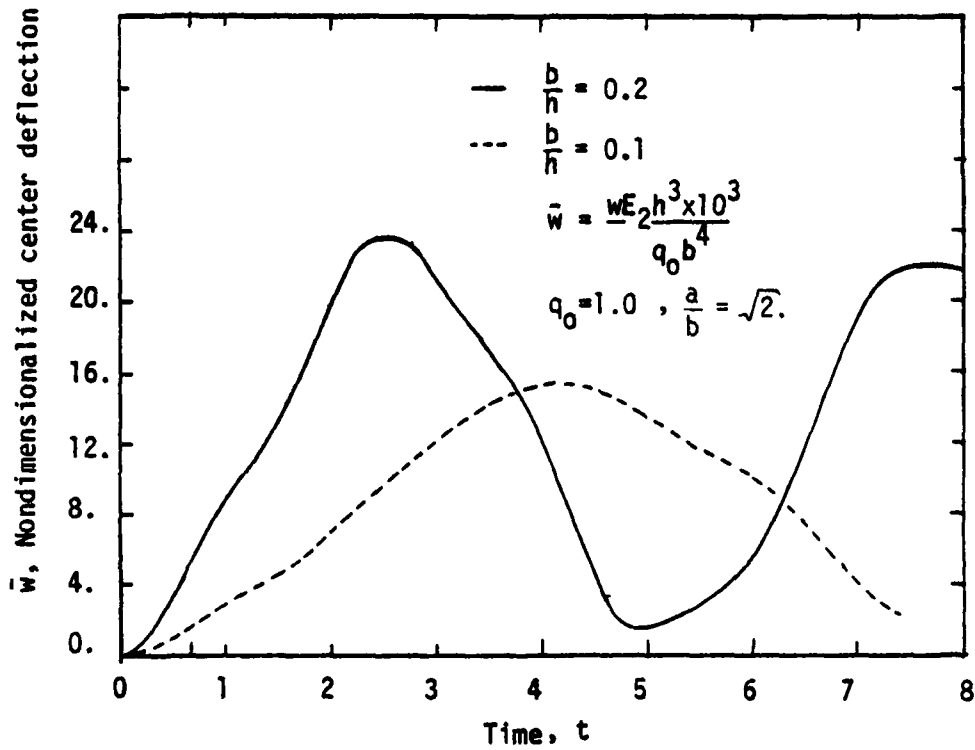


Figure 6. Effect of plate thickness on the transient response of orthotropic plates (see Figure 5 for material properties) under suddenly applied patch loading (i.e., load on the square area at the center of the rectangular plate).

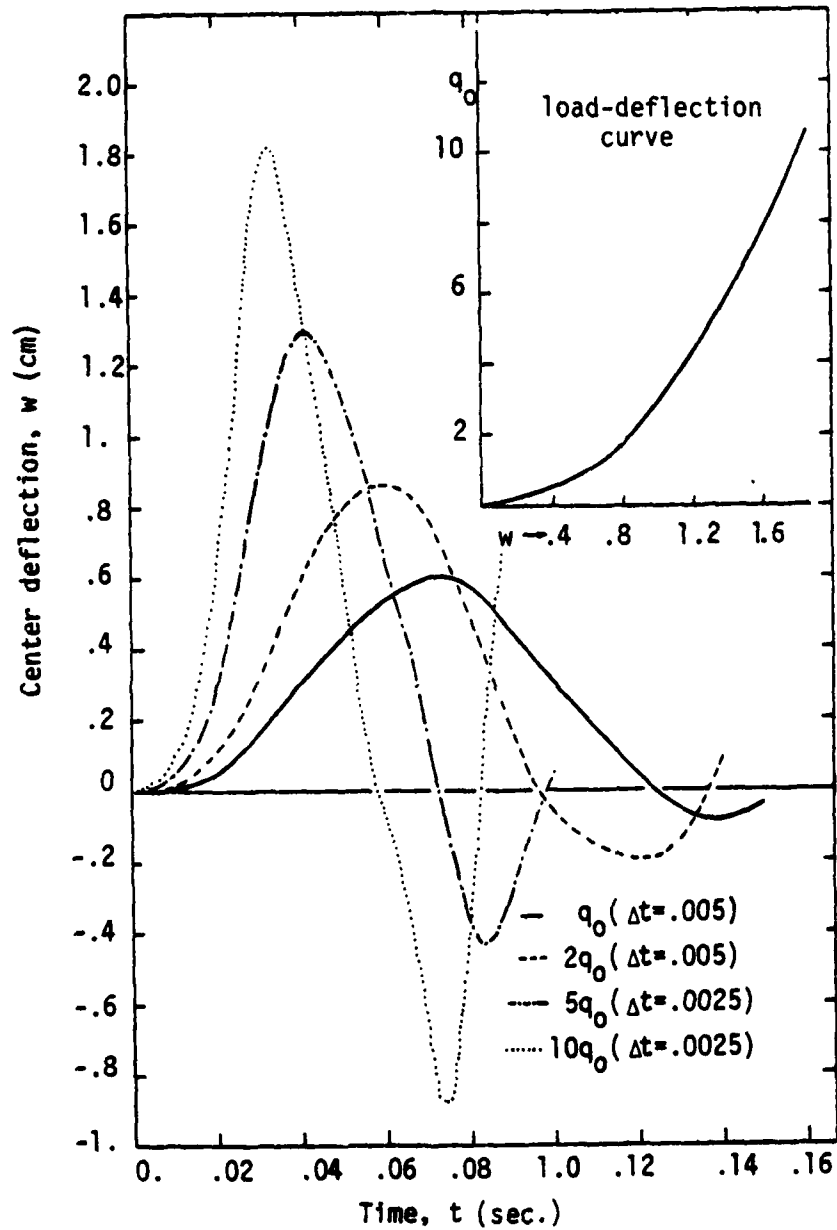


Figure 7. Nonlinear transient response of isotropic plates (see eqn. (23) and Figure 2 for the data and finite element mesh and boundary conditions) under suddenly applied uniformly distributed loads.

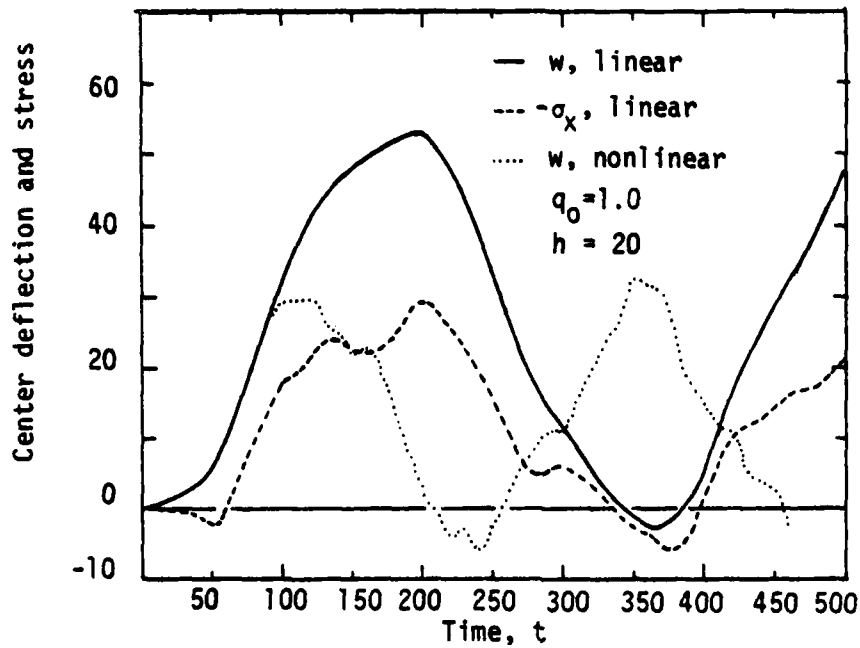
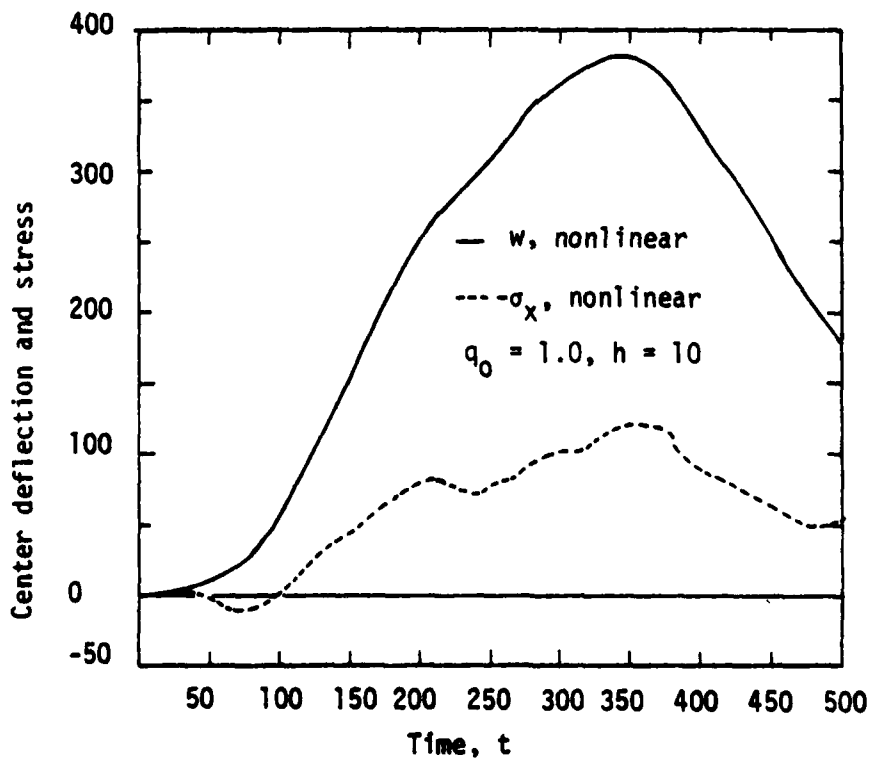
(a) Clamped circular plate, $h = 20$ ".(b) Clamped circular plate, $h = 10$ ".

Figure 8. Transient response of a clamped, isotropic, circular plate under suddenly applied transverse load (see Figure 3 for the finite-element mesh and boundary conditions).

Figure 8a also contains plots of center deflection of the linear and nonlinear analysis. The effect of the (von Karman type) nonlinearity is to decrease the amplitude and period of the center deflection and stress.

The results of the nonlinear analysis of layered composite plates are presented next. Figures 9 and 10 contain plots of the center deflection versus time for simply supported (BC1) two-layer cross-ply $[0^\circ/90^\circ]$ and angle-ply $[45^\circ/-45^\circ]$ plates, respectively. The same data (except for the material properties) as in Eq. (22) is employed. The effect of coupling between the inplane displacements and bending deflections is to increase the amplitude of the center deflection in the linear analysis. Figure 10 also contains the results of uniformly loaded angle-ply plates. It is apparent from this figure that as the load is changed from uniformly distributed to patch loading, the response curves change from a regular to irregular curve (and for point loading the response becomes spiky).

The plots of the center deflection versus time for single-layer (0°), cross-ply $[0^\circ/90^\circ]$, and angle-ply $[45^\circ/-45^\circ]$ square plates under suddenly applied uniform loading are presented in Figs. 11 and 12, respectively; 2×2 (uniform) mesh with 5 DOF is used. The boundary conditions used in this set of problems (BC2) are different from the simply supported boundary conditions (BC1) used earlier: the two types of boundary conditions are shown in Fig. 2. The data used is the same as that in Eq. (23) (except for the material properties). The effect of the nonlinearity and the lamination scheme on the amplitude and period of the center deflection is apparent from the results. Note that the rate of increase in the amplitude of the center deflection decreases

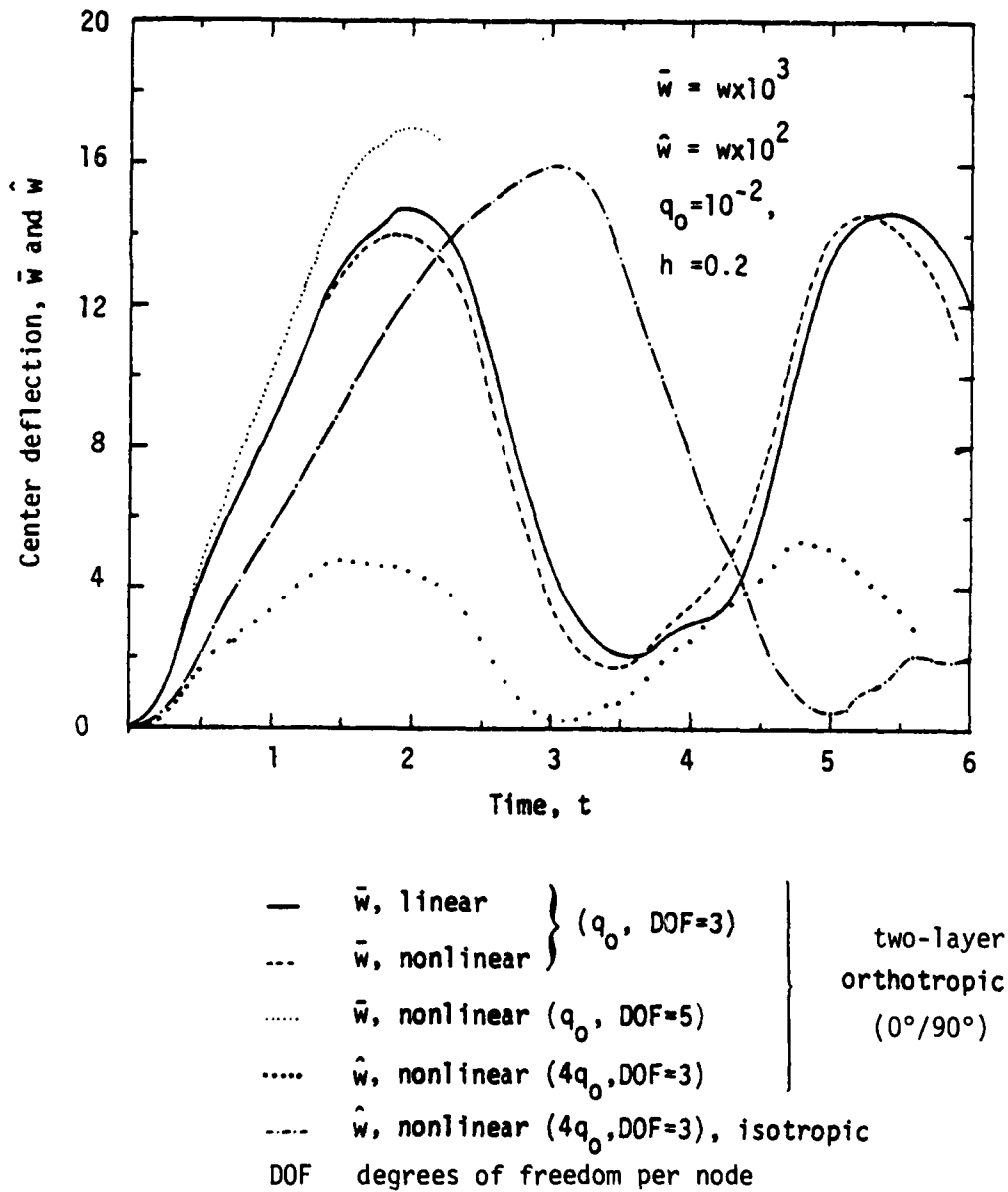


Figure 9. Transient response of two-layer cross-ply ($0^\circ/90^\circ$) rectangular plates under suddenly applied patch loading (see eqn.(22) and Figure 1 for the data and mesh information; see Figure 5 for the material properties).

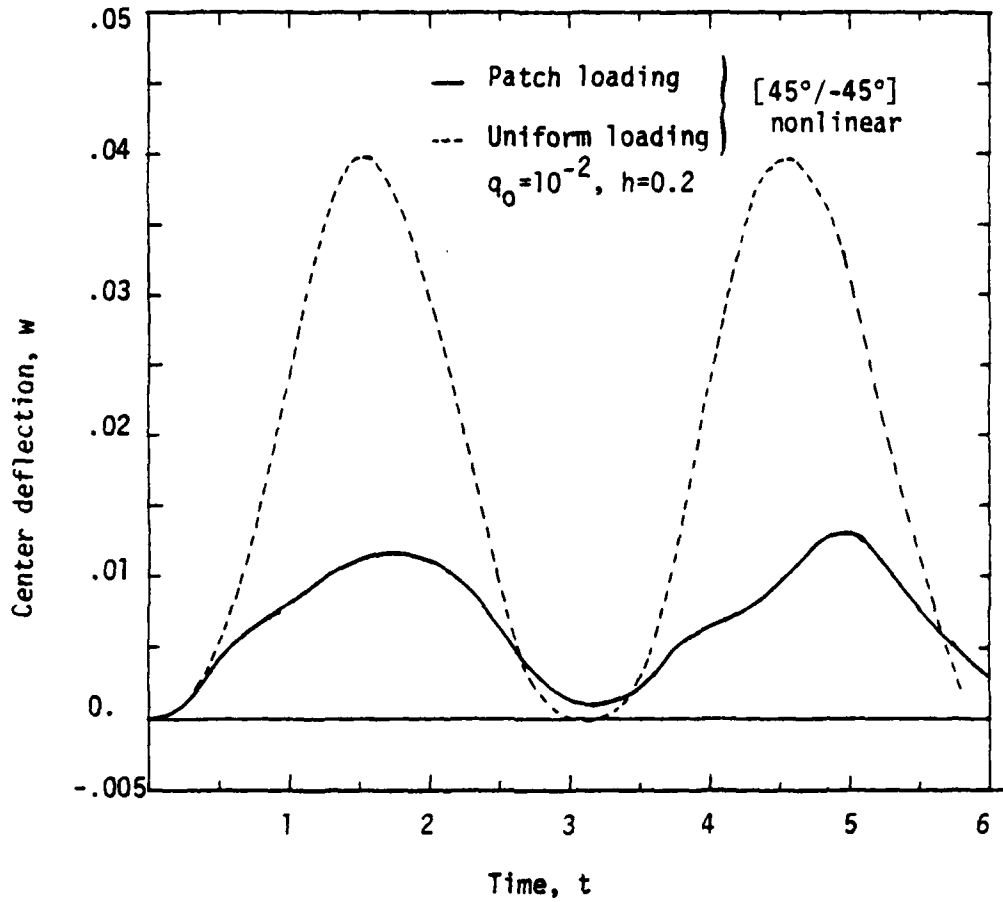


Figure 10. Nonlinear transient response of two-layer angle-ply $[45^\circ/-45^\circ]$ rectangular plates under suddenly applied patch loading (see eqn. (22) and Figure 1 for data).

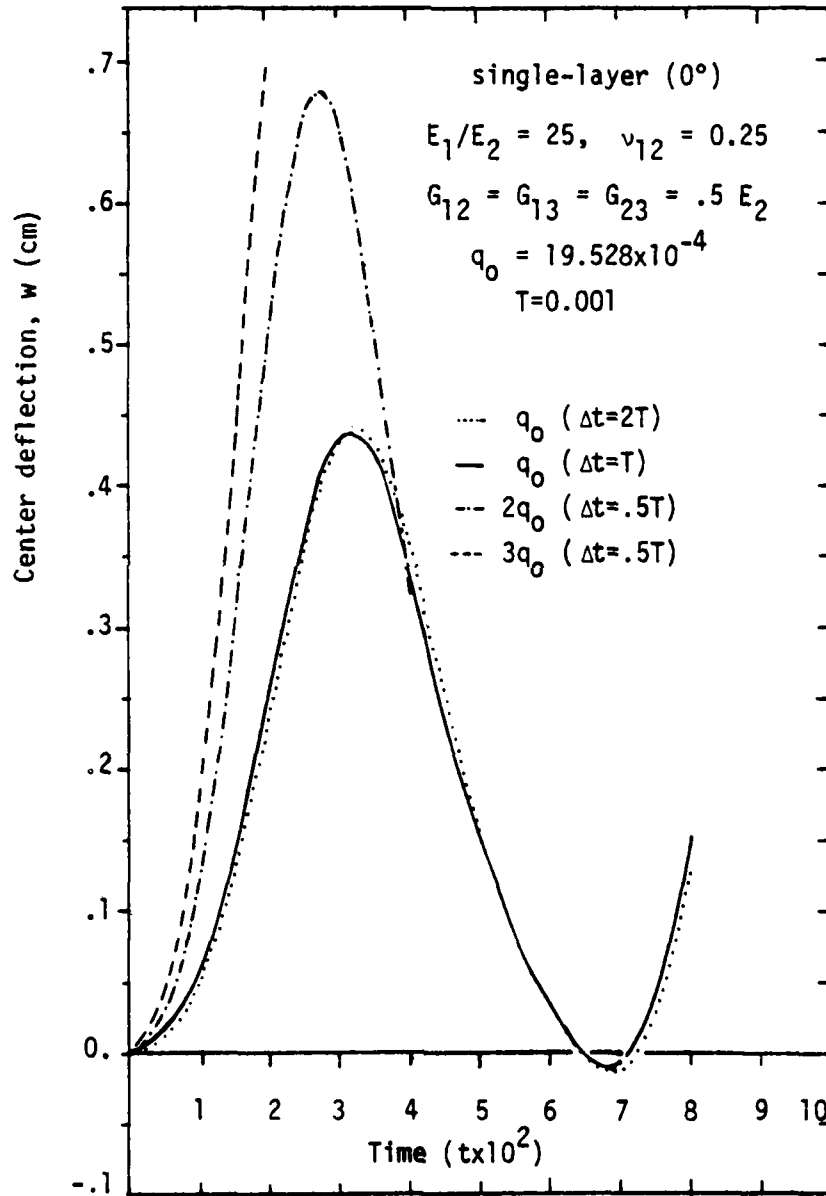


Figure 11. Nonlinear transient response of single-layer (0°) orthotropic square plates under suddenly applied pressure loading (see eqn. (23) and Figure 2 for the data and mesh); BC2 boundary conditions were used.

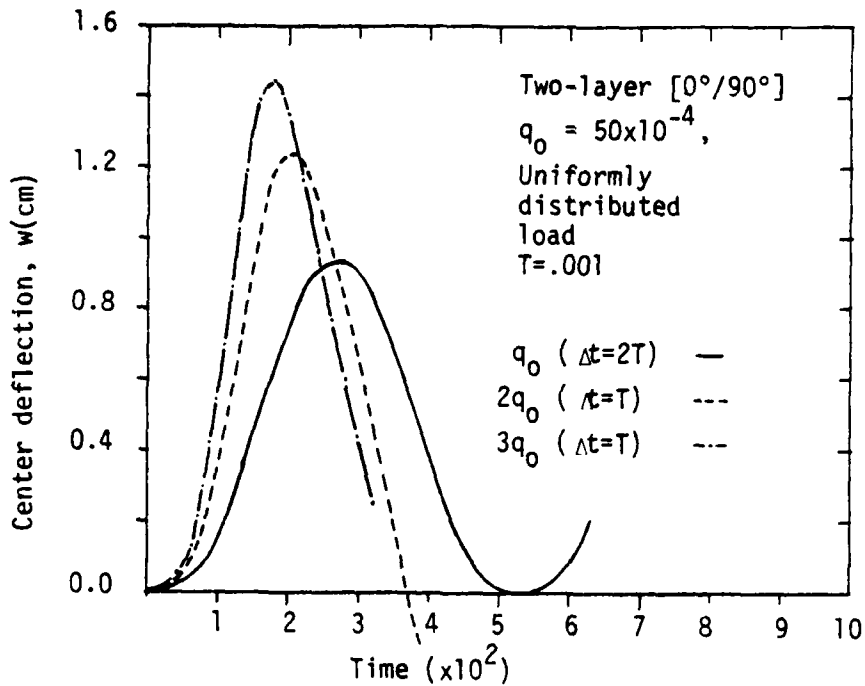
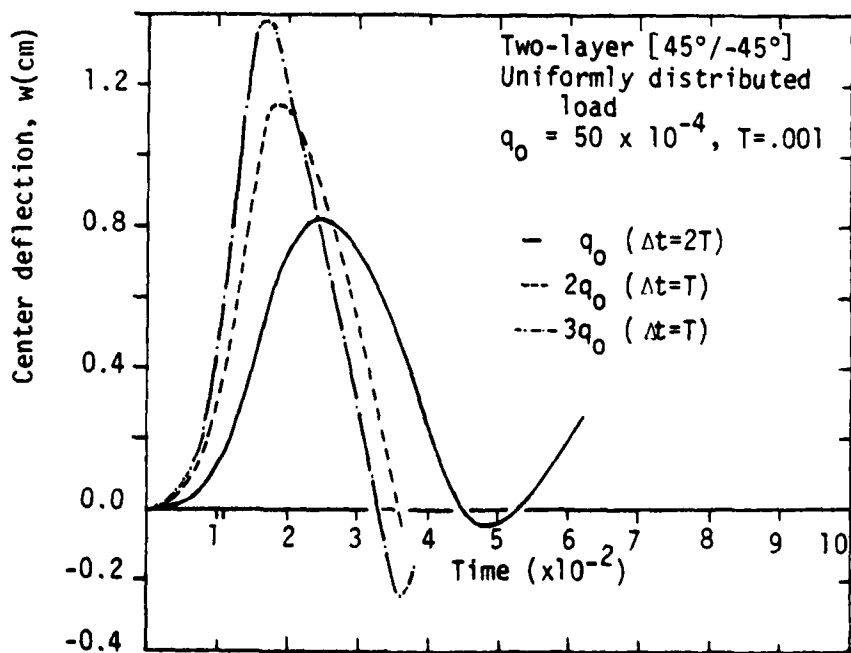
(a) Cross-ply $[0^\circ/90^\circ]$ plates(b) Angle-ply $[45^\circ/-45^\circ]$ plates

Figure 12. Nonlinear transient response of laminated square plates under suddenly applied uniform loading (see Figure 10 for other information).

with increasing load. Further note that the maximum center deflection for the cross-ply plates is about 10% larger than that of the angle-ply $[45^\circ/-45^\circ]$ plates.

Lastly, the effect of boundary conditions (BC1 and BC2) on the center deflection of two-layer square plates under uniformly distributed load was investigated; Figure 13 contains results of the investigation. It is clear that the response of cross-ply as well as angle-ply plates under BC1 differ significantly from the results of plates under BC2. Note also that suppression of the inplane degrees freedom results in about 50% decrease in the center deflection of angle-ply $[45^\circ/-45^\circ]$ plates.

Summary and Conclusions

A shear flexible finite element that accounts for the von Karman strains is employed in the transient analysis of layered composite plates. The present results for isotropic plates are very close to the analytical and other finite element solutions available in the literature. The present results of layered composite plates should serve as reference solutions for future investigations. Although the paper contains results for certain geometries, loadings, lamination scheme, and material properties, it should be pointed out that the element developed herein can be employed to laminated plates of arbitrary geometry, lamination scheme, material properties, boundary conditions, and loading (only limitations are those implied in the laminated plate theory used). The present analysis does not account for material damping effects; studies of composite plates accounting for material damping and material nonlinearities are awaiting attention.

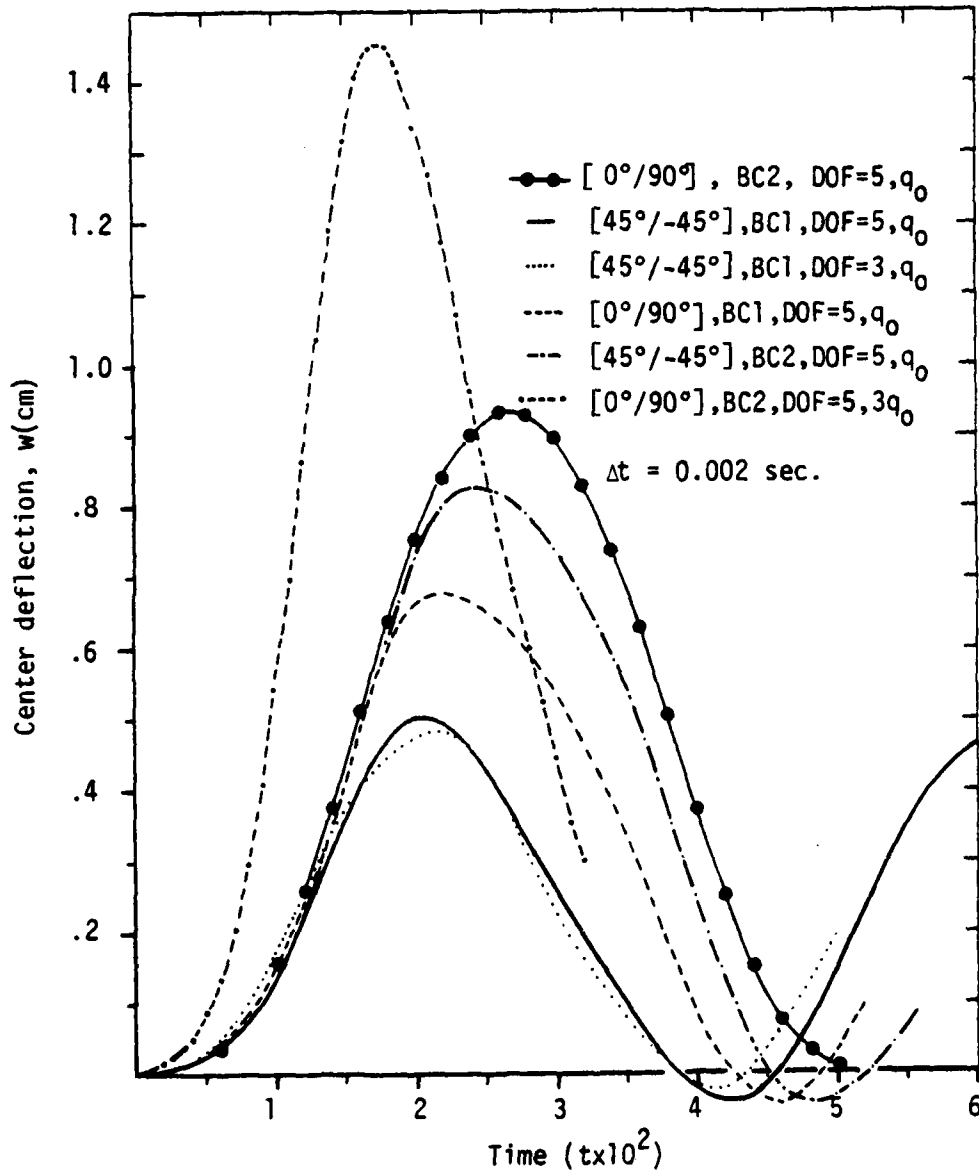


Figure 13. Effect of the boundary conditions (BC1 and BC2) on the nonlinear transient response of laminated square plates under suddenly applied transverse, uniformly distributed, loading (see eqn. (23) for the data and Figure 2 for the mesh and boundary conditions; orthotropic properties of layers are given in Figure 11).

Acknowledgments

The results reported in the paper were obtained during an investigation supported by Structural Mechanics Program of the Air Force Office of Scientific Research (Grant AFOSR-81-0142). The author is grateful to Dr. Anthony Amos (AFOSR) for his encouragement and support of this work. Sincere thanks are also due to Professor R. M. Jones for his comments, which lead to an improved manuscript.

References

1. Lamb, H., "On Waves in an Elastic Plate," Proc. Royal Soc. London, Series A, Vol. 93, 1917, p. 114
2. David, N., and Lawhead, W., "Transient Analysis of Oblique Impact on Plates," J. Mech. Phys. Solids, Vol. 13, 1965, p. 199.
3. Timoshenko, S., "On the Correction for Shear of the Differential Equation for Transverse Vibrations of Prismatic Bars," Phil. Mag., Series 6, Vol. 41, 1921, p. 744
4. Reissner, E., "The Effect of Transverse Shear Deformation on the Bending of Elastic Plates," J. Appl. Mech., Trans. ASME, Vol. 67, 1945, p. A-69.
5. Reissner, E., "On Bending of Elastic Plates," Q. Appl. Math., Vol. 5, 1947, p. 55.
6. Mindlin, R. D., "Influence of Rotatory Inertia and Shear on Flexural Motions of Isotropic, Elastic Plates," J. Appl. Mech., Vol. 18, 1951, p. 31.
7. Yang, P. C., Norris, C. H., and Stavsky, Y., "Elastic Wave Propagation in Heterogeneous Plates," Int. J. Solids Struct., Vol. 2, 1966, pp. 665-684.
8. Medwadowski, S. J., "A Refined Theory of Elastic, Orthotropic Plates," J. Appl. Mech., Vol. 25, 1958, pp. 437-443.
9. Ebcioğlu, I. K., "A Large Deflection Theory of Anisotropic Plates," Ingenieur-Archiv, Vol. 33, 1964, pp. 396-403.
10. Moon, F. C., "Wave Surfaces Due to Impact on Anisotropic Plates," J. Compos. Mater., Vol. 6, 1972, pp. 62-79.
11. Moon, F. C., "One-Dimensional Transient Waves in Anisotropic Plates," J. Appl. Mech., Vol. 40, 1973, pp. 485-490.

12. Chow, T. S., "In the Propagation of Flexural Waves in an Orthotropic Laminated Plate and its Response to an Impulsive Load," J. Compos. Mater., Vol. 5, 1971, pp. 306-319.
13. Wang, A. S. D., Chou, P. C., and Rose, J. L., "Strongly Coupled Stress Waves in Heterogeneous Plates," AIAA J., 1972, pp. 1088-1090.
14. Sun, C. T. and Whitney, J. M., "Dynamic Response of Laminated Composite Plates," AIAA J., Vol. 13, No. 10, 1975, pp. 1250-9-1260.
15. Whitney, J. M. and Sun, C. T., "Transient Response of Laminated Composite Plates Subjected to Transverse Dynamic Loading," J. Acoust. Soc. Am., Vol. 61, No. (1), 1977, pp. 101-104.
16. Reddy, J. N., "On the Solutions to Forced Motions of Layered Composite Plates," J. Applied Mechanics, to appear.
17. Reddy, J. N., "Dynamic (Transient) Analysis of Layered Anisotropic Composite-Material Plates," Int. J. Numer. Meth. Engng., to appear.
18. Hinton, E., Owen, D. R. J., and Shantaram, D., "Dynamic Transient Linear and Nonlinear Behavior of Thick and Thin Plates," in The Mathematics of Finite Elements and Applications II, J. R. Whitteman (ed.), Academic Press, London, 1976.
19. Hinton, E., "The Dynamic Transient Analysis of Axisymmetric Circular Plates by the Finite Element Method," J. Sound and Vibration, Vol. 46, 1976, pp. 465-472.
20. Pica, A., and Hinton, E., "Transient and Pseudo-Transient Analysis of Mindlin Plates," Int. J. Numer. Meth. Engng., Vol. 15, 1980, pp. 189-208.
21. Akay, H. U., "Dynamic Large Deflection Analysis of Plates Using Mixed Finite Elements," Computers & Structures, Vol. 11, 1980, pp. 1-11.
22. Jones, R. M., Mechanics of Composite Materials, McGraw-Hill, New York, 1975.
23. Reddy, J. N., "A Penalty Plate-Bending Element for the Analysis of Laminated Anisotropic Composite Plates," Int. J. Num. Meth. Engng., Vol. 15, 1980, pp. 1187-1206.
24. Bathe, K. J., and Wilson, E. L., Numerical Methods in Finite Element Analysis, Prentice-Hall, Englewood Cliffs, NJ, 1976.
25. Leech, J. W., "Stability of Finite Difference Equations for the Transient Response of a Flat Plate," AIAA J., Vol. 3, No. 9, 1965, pp. 1772-1773.
26. Tsui, T. Y., and Tong, P., "Stability of Transient Solution of Moderately Thick Plate by Finite Difference Method," AIAA J., Vol. 9, 1971, pp. 2062-2063.

27. Reismann, H. and Lee, Y., "Forced Motions of Rectangular Plates," in Developments in Theoretical and Applied Mechanics, Vol. 4, (Ed. D. Frederick), Pergamon Press, New York, 1969, pp. 3-18.

APPENDIX A : ELEMENTS OF STIFFNESS AND MASS MATRICES

stiffness matrix:

$$[K] = \begin{bmatrix} [K^{11}] & [K^{12}] & [K^{13}] & [K^{14}] & [K^{15}] \\ [K^{21}] & [K^{22}] & [K^{23}] & [K^{24}] & [K^{25}] \\ [K^{31}] & [K^{32}] & [K_1^{33}] & [K_1^{34}] & [K_1^{35}] \\ & & + [K_2^{33}] & + [K_2^{34}] & + [K_2^{35}] \\ [K^{41}] & [K^{42}] & [K_1^{43}] & [K^{44}] & [K^{45}] \\ & & + [K_2^{43}] & & \\ [K^{51}] & [K^{52}] & [K_1^{53}] & [K^{54}] & [K^{55}] \\ & & + [K_2^{53}] & & \end{bmatrix}$$

mass matrix

$$[M] = \begin{bmatrix} P[S] & [0] & [0] & R[S] & [0] \\ [0] & P[S] & [0] & [0] & R[S] \\ [0] & [0] & P[S] & [0] & [0] \\ R[S] & [0] & [0] & I[S] & [0] \\ [0] & R[S] & [0] & [0] & I[S] \end{bmatrix}$$

The matrix coefficients $K_{ij}^{\alpha\beta}$ are given by

$$[K^{11}] = A_{11}[S^{xx}] + A_{16}([S^{xy}] + [S^{xy}]^T) + A_{66}[S^{yy}],$$

$$[K^{12}] = A_{12}[S^{xy}] + A_{16}[S^{xx}] + A_{26}[S^{yy}] + A_{66}[S^{xy}]^T \\ = [K^{21}]^T,$$

$$[K^{13}] = A_{11}[R_x^{xx}] + A_{12}[R_y^{xy}] + A_{16}([R_x^{xy}] + [R_x^{xy}]^T \\ + [R_y^{xx}]) + A_{26}[R_y^{yy}] + A_{66}([R_y^{xy}]^T + [R_x^{yy}]) = \frac{1}{2}[K^{31}]^T,$$

$$[K^{14}] = B_{11}[S^{xx}] + B_{16}([S^{xy}] + [S^{xy}]^T) + B_{66}[S^{yy}] = [K^{41}]^T,$$

$$\begin{aligned} [K^{15}] &= B_{12}[S^{xy}] + B_{16}[S^{xx}] + B_{26}[S^{yy}] + B_{66}[S^{xy}]^T \\ &= [K^{51}]^T, \end{aligned}$$

$$[K^{22}] = A_{22}[S^{yy}] + A_{26}([S^{xy}]^T + [S^{xy}]) + A_{66}[S^{xx}],$$

$$\begin{aligned} [K^{23}] &= A_{12}[R_x^{xy}]^T + A_{22}[R_y^{yy}] + A_{26}([R_y^{xy}]^T + [R_y^{xy}] \\ &\quad + [R_x^{yy}]) + A_{16}[R_x^{xx}] + A_{66}([R_x^{xy}]^T + [R_y^{xx}]) \\ &= \frac{1}{2} [K^{32}]^T, \end{aligned}$$

$$\begin{aligned} [K^{24}] &= B_{12}[S^{xy}]^T + B_{26}[S^{yy}] + B_{16}[S^{xx}] + B_{66}[S^{xy}] \\ &= [K^{42}]^T, \end{aligned}$$

$$\begin{aligned} [K^{25}] &= B_{22}[S^{yy}] + B_{26}([S^{xy}] + [S^{xy}]^T) + B_{66}[S^{xx}] \\ &= [K^{52}]^T, \end{aligned}$$

$$[K_1^{33}] = A_{55}[S^{xx}] + A_{45}([S^{xy}] + [S^{xy}]^T) + A_{44}[S^{yy}],$$

$$\begin{aligned} [K_2^{33}] &= \frac{1}{2} \int_{Re} [\bar{N}_1 \frac{\partial \phi_i}{\partial x} \frac{\partial \phi_j}{\partial x} + \bar{N}_6 (\frac{\partial \phi_i}{\partial x} \frac{\partial \phi_j}{\partial y} + \frac{\partial \phi_i}{\partial y} \frac{\partial \phi_j}{\partial x}) \\ &\quad + \bar{N}_2 \frac{\partial \phi_i}{\partial y} \frac{\partial \phi_j}{\partial y}] dx dy, \end{aligned}$$

$$[K_1^{34}] = A_{55}[S^{x0}] + A_{45}[S^{y0}] = [K_1^{43}]^T,$$

$$\begin{aligned} [K_2^{34}] &= B_{11}[R_x^{xx}] + B_{16}([R_x^{xy}] + [R_x^{xy}]^T + [R_y^{xx}]) \\ &\quad + B_{12}[R_y^{xy}]^T + B_{26}[R_y^{yy}] + B_{66}([R_x^{yy}] + [R_y^{xy}]) \\ &= 2[K_2^{43}]^T, \end{aligned}$$

$$[K_1^{35}] = A_{45}[S^{x0}] + A_{44}[S^{y0}] = [K_1^{53}]^T,$$

$$[K_2^{35}] = B_{12}[R_x^{xy}] + B_{16}[R_x^{xx}] + B_{22}[R_y^{yy}] + B_{26}([R_y^{xy}]^T +$$

$$[R_x^{yy}] + [R_y^{xy}]) + B_{66}([R_x^{xy}]^T + [R_y^{xx}]) = 2[K^{53}]^T,$$

$$[K^{44}] = D_{11}[S^{xx}] + D_{16}([S^{xy}] + [S^{xy}]^T) + D_{66}[S^{yy}] +$$

$$+ A_{55}[S],$$

$$[K^{45}] = D_{12}[S^{xy}] + D_{16}[S^{xx}] + D_{26}[S^{yy}] + D_{66}[S^{xy}]^T +$$

$$+ A_{45}[S] = [K^{54}]^T,$$

$$[K^{55}] = D_{26}([S^{xy}] + [S^{xy}]^T) + D_{66}[S^{xx}] + D_{22}[S^{yy}] +$$

$$+ A_{44}[S].$$

and

$$S_{ij}^{\xi\eta} = \int_{R^e} \frac{\partial \phi_i}{\partial \xi} \frac{\partial \phi_j}{\partial \eta} dx dy, \quad \xi, \eta = 0, x, y, \quad S_{ij}^{00} \equiv S_{ij},$$

$$R_{\zeta}^{\xi\eta} = \int_{R^e} \frac{1}{2} \left(\frac{\partial w}{\partial \zeta} \right) \frac{\partial \phi_i}{\partial \xi} \frac{\partial \phi_j}{\partial \eta} dx dy, \quad \zeta, \xi, \eta = 0, x, y,$$

$$\bar{N}_1 = A_{11} \left(\frac{\partial w}{\partial x} \right)^2 + A_{12} \left(\frac{\partial w}{\partial y} \right)^2 + 2A_{16} \frac{\partial w}{\partial x} \frac{\partial w}{\partial y},$$

$$\bar{N}_2 = A_{12} \left(\frac{\partial w}{\partial x} \right)^2 + A_{22} \left(\frac{\partial w}{\partial y} \right)^2 + 2A_{26} \frac{\partial w}{\partial x} \frac{\partial w}{\partial y},$$

$$\bar{N}_6 = A_{16} \left(\frac{\partial w}{\partial x} \right)^2 + A_{26} \left(\frac{\partial w}{\partial y} \right)^2 + 2A_{66} \frac{\partial w}{\partial x} \frac{\partial w}{\partial y}.$$

UNCLASSIFIED

SECURITY CLASSIFICATION OF THIS PAGE (When Data Entered)

REPORT DOCUMENTATION PAGE		READ INSTRUCTIONS BEFORE COMPLETING FORM
1. REPORT NUMBER VPI-E-82.8	2. GOVT ACCESSION NO. AD-A113852	3. RECIPIENT'S CATALOG NUMBER
4. TITLE (and Subtitle) GEOMETRICALLY NONLINEAR TRANSIENT ANALYSIS OF LAMINATED COMPOSITE PLATES		5. TYPE OF REPORT & PERIOD COVERED Interim
		6. PERFORMING ORG. REPORT NUMBER Tech. Reprt No. AFOSR-81-3
7. AUTHOR(s) J. N. Reddy		8. CONTRACT OR GRANT NUMBER(s) AFOSR-81-0142
9. PERFORMING ORGANIZATION NAME AND ADDRESS Virginia Polytechnic Institute and State University Blacksburg, Virginia 24061		10. PROGRAM ELEMENT, PROJECT, TASK AREA & WORK UNIT NUMBERS 81-00707
11. CONTROLLING OFFICE NAME AND ADDRESS United States Air Force Air Force Office of Scientific Research Bldg. 410, Bolling AFB, D.C. 20332		12. REPORT DATE March 1982
14. MONITORING AGENCY NAME & ADDRESS (if different from Controlling Office)		13. NUMBER OF PAGES 34
		15. SECURITY CLASS. (of this report) UNCLASSIFIED
		15a. DECLASSIFICATION DOWNGRADING SCHEDULE
16. DISTRIBUTION STATEMENT (of this Report) This document has been approved for public release and sale; distribution unlimited.		
17. DISTRIBUTION STATEMENT (of the abstract entered in Block 20, if different from Report)		
18. SUPPLEMENTARY NOTES A portion of this report will be presented at the International Conference on Finite Element Methods, August 2-6, 1982, Shanghai, China; the paper is submitted to an archive journal.		
19. KEY WORDS (Continue on reverse side if necessary and identify by block number) angle-ply, composite materials, cross-ply, fiber-reinforced materials, finite element results, geometric nonlinearity, laminates, plates, rectangular plates transient analysis, transverse shear deformation.		
20. ABSTRACT (Continue on reverse side if necessary and identify by block number) Forced motions of laminated composite plates are investigated using a finite element that accounts for the transverse shear strains, rotary inertia, and large rotations (in the von Karman sense). The present results when specialized for isotropic plates are found to be in good agreement with those available in the literature. Numerical results of the nonlinear analysis are presented showing the effects of plate thickness, lamination scheme, boundary conditions, and loading on the deflections and stresses. The new results for composite plates should serve as bench marks for future investigations.		